Available online at www.sciencedirect.com

SciVerse ScienceDirect

journal homepage: www.elsevier.com/locate/he

High-rate discharge characteristics of metal hydride modified by electroless nickel plating based on experimental design approach

Sheng-Han Lin [a], *Wu-Tsan Wu* [b], *Jing-Shan Do* [b,*]

[a] *Department of Chemical Engineering and Materials Engineering, Tunghai University, Taichung 407, Taiwan*
[b] *Department of Chemical Engineering and Materials Engineering, National Chin-Yi University of Technology, Taichung County 411, Taiwan*

ARTICLE INFO

Article history:
Received 4 August 2011
Received in revised form
12 October 2011
Accepted 17 October 2011
Available online 12 November 2011

Keywords:
Metal hydride
Surface modification
Electroless plating
Nickel
Experimental design

ABSTRACT

In this study, a metal hydride (MH) alloy ($MmNi_{3.81}Mn_{0.41}Al_{0.19}Co_{0.76}$) is modified by electroless nickel plating with the controlled variables of plating time (A), temperature (B), amount of MH alloy (C), pH (D), concentration of reducing agent ($NaH_2PO_2 \cdot H_2O$) (E), and complex agent ($Na_3C_6H_5O_7 \cdot 2H_2O$) (F). Based on the two-level orthogonal array strategy, the Ni loadings on the modified MH alloy of −20.25–11.83% are strongly affected by the variables of A, D, E, and F, as well as the two-factor interactions of AB, AC, AD, BD, and EF. The utility of the unmodified MH alloy used as the negative electrode material of the Ni–MH battery decreases from 100.6 to 7.6% when increasing the discharge rate from 0.2 to 10 C. The utility at the discharge rate of 10 C can be increased to 54.5% for the MH alloy modified by electroless plating Ni when the plating time, temperature, amount of MH, pH, and concentrations of the reducing agent and complex agent are equal to 10 min, 70 °C, 2 g, 7.0, 15 g L^{-1}, and 30 g L^{-1}, respectively.

Copyright © 2011, Hydrogen Energy Publications, LLC. Published by Elsevier Ltd. All rights reserved.

1. Introduction

In recent years, microgrids for small communities have been proposed and developed for decentralized electricity generation. Microgrid systems can also be easily integrated with renewable energies such as photovoltaic arrays or wind turbines [1]. The nickel–metal hydride (Ni–MH) battery is one promising energy storage device for microgrids due to its good energy and power efficiencies, flexible design capability for demands, and environmentally friendly nature. Furthermore, the Ni–MH battery has also been widely used for hybrid electric vehicles (HEVs) [2]. However, the properties of Ni–MH batteries, such as a high charge/discharge rate, should be further improved to increase their performance in wide applications.

The charge/discharge performances of Ni–MH batteries are generally governed by the electrochemical properties of the MH alloy. Hence, many efforts have been given to promote the electrochemical activity of the MH alloy. Metal hydrides are frequently modified by electroless plating copper [3–7], cobalt [3,8], nickel [3,5,9–14], palladium [5], and alloys [15] to improve their electrochemical properties. The surfaces of metal hydrides can also be modified by ball milling [16–24], vacuum evaporation plating [25–27], and electroplating [28] techniques. The exchange current increases from 670 mA g^{-1} for pristine $LaNi_{4.7}Al_{0.3}$–750 mA g^{-1} for Cu-coated $LaNi_{4.7}Al_{0.3}$, and the discharge capacity is also promoted by electroless plating Cu [4]. The discharge capacity and high-rate discharge properties of metal hydrides can be effectively improved by microencapsulation of metals such as Ni

* *Corresponding author*. Fax: +886 4 3926617.
E-mail address: jsdo@ncut.edu.tw (J.-S. Do).

0360-3199/$ – see front matter Copyright © 2011, Hydrogen Energy Publications, LLC. Published by Elsevier Ltd. All rights reserved.
doi:10.1016/j.ijhydene.2011.10.083

and Cu [4,29-31], which are softer than hydrogen storage alloys, to provide the necessary contact of powders and good electric and thermal conductions [4,29]. When $MmNi_{3.25}Al_{0.35}Mn_{0.25}Co_{0.66}$ is coated with Cu, Ni–P, and Co–P by the electroless plating technique, the Cu-coated alloy exhibits the best discharge capacity [3]. The performance of the $MmNi_{2.38}Al_{0.82}Co_{0.66}Si_{0.77}Fe_{0.13}Mn_{0.24}$ alloy increases by 15% by electroless plating of a thin layer of Co [8]. The initial and maximum capacities of $Ti_{0.35}Zr_{0.35}Ni_{1.2}V_{0.6}Mn_{0.2}Cr_{0.2}$ and $MmB_{4.3}(Al_{0.3}Mn_{0.4})_{0.5}$ (Mm = La-rich misch metal, B = Co, Mo, Mn, Al, Cu) are improved by treating these materials with KOH aqueous solution, followed by electroless plating nickel [12]. The high-rate performances of $Ti_{0.35}Zr_{0.35}Ni_{1.2}V_{0.6}Mn_{0.2}Cr_{0.2}$ and $MmB_{4.3}(Al_{0.3}Mn_{0.4})_{0.5}$ are also promoted when modified by electroless plating nickel [12,13].

For MH alloys modified by electroless plating metal (such as Ni), the effect of electroless coating factors on the metal loading and the charge/discharge properties of alloys are generally complicated. The ability to understand the single and mutual effects of these factors is hence limited to conventional experimental strategies. Experimental design and optimization provide a powerful tool for studying complex systems with mutual effects by using a limited number of experiments [32]. The two-level orthogonal array strategy is used for studying the charge/discharge properties of $MmNi_{3.81}Mn_{0.41}Al_{0.19}Co_{0.76}$ modified by electroless plating Ni–P. The effect of single and mutual electroless plating factors on Ni loadings and the utility of the modified alloy are systematically studied.

2. Experimental

2.1. Electroless coating of metal hydride

Suitable amount of metal hydride ($MmNi_{3.81}Mn_{0.41}Al_{0.19}Co_{0.76}$) alloy powder (NEXCELL Battery Co., Ltd.) was added into a 100 ml aqueous solution containing 30 g L^{-1} nickel chloride, 20 g L^{-1} ammonium hydrogen bifluoride, 10 g L^{-1} potassium acetate, and suitable concentrations of trisodium citrate (complex agent) and sodium hypophosphite (reducing agent). The reaction time (A), reaction temperature (B), amount of metal hydride (C), pH (D), concentration of reducing agent (E), and concentration of complex agent (F) were chosen as the variables for the two-level orthogonal array design. The high and low levels of these six factors are given in Table 1. The as-modified MH alloys were filtrated and washed with deionized (DI) water several times and then dried in an 80 °C vacuum oven for 1 h. The loadings of Ni and P on the modified MH alloys were analyzed by atomic adsorption spectroscopy (AAS) and energy dispersive spectroscopy (EDS), respectively. The surface morphology of the as-modified MH alloy powder was analyzed by SEM.

Table 1 – Factors and levels of the orthogonal array.

Factors	Low level	High level
A, run time/min	10	40
B, reaction temperature/°C	70	90
C, weight of MH/g	2	4
D, pH	3.0	7.0
E, $[NaH_2PO_2 \cdot H_2O]$/g L^{-1}	15	30
F, $[Na_3C_6H_5O_7 \cdot 2H_2O]$/g L^{-1}.	10	30

2.2. Preparation and characterization of MH as negative electrode of Ni–MH battery

0.5 g polyvinyl alcohol (PVA) powder was dissolved in 6 ml DI water as the PVA solution. The metal hydride slurry, which was prepared by mixing 0.7 g MH alloy powder with 0.7 ml DI water, 0.7 ml methanol, and 56 μl PVA solution, was uniformly brushed onto a 1.5 cm × 1.75 cm Ni-foam (1.6 mm thickness, NEXCELL Battery Co., Ltd.). After drying at 70 °C for 1 h, the MH negative electrode was pressed under a pressure of 50 kg cm^{-2}.

The as-prepared MH negative electrode placed among two Ni hydroxide positive plate electrodes (NEXCELL Battery Co., Ltd.) was separated by polypropylene (PP) films, and then, two PMMA plates were used to press the electrodes tightly with four screws as illustrated in Fig. 1(a). The flooded Ni–MH battery was fabricated by immersing the electrode assembly into a 70 ml 8.02 M KOH and 0.477 M LiOH aqueous solution (Fig. 1(b)). The electrochemical properties of the homemade Ni–MH batteries were limited by the MH negative electrode, because the theoretical capacity of the two Ni hydroxide positive electrodes was significantly greater than that of the MH negative electrode. The homemade Ni–MH batteries were galvanostatically charged to 160% SOC (state of charge) at 0.2 C and then discharged to 0.95 V at the same C-rate in order to activate the batteries to stable capacities. As for the activated batteries, they were charged to 140% SOC at 0.2 C and then discharged at various C-rates to the sharp change in voltage.

3. Results and discussion

Two-level orthogonal array strategy used for studying the charge/discharge properties of $MmNi_{3.81}Mn_{0.41}Al_{0.19}Co_{0.76}$ modified by electroless plating Ni–P is used to obtaining the optimal Ni plating conditions. The orthogonal array strategy is proposed and developed by Taguchi, which is a commonly adopted approach for optimizing the experimental parameters [33]. The experimental conditions are laid out as an orthogonal array (table). Using the orthogonal array, the experimental design is straightforward and consistent. Then the overall testing time and the experimental costs are reduced [33]. The fundamental theory and techniques as well as the orthogonal arrays of the Taguchi method are summarized in the literatures [33,34]. Firstly six factors with low and high levels are chosen (Table 1), then the experiments based a suitable two-level orthogonal array are performed. Using the Ni loading and utility of MH alloy as the responses, the approximate statistical analysis is evaluated with Statistical Analysis System (SAS) software, and discussed in the following sections.

3.1. Modification of MH by electroless plating Ni–P

The orthogonal array $L_{16}(2^{15})$ was designed for investigating the effects of control factors A, B, C, D, E and F, and two-factor

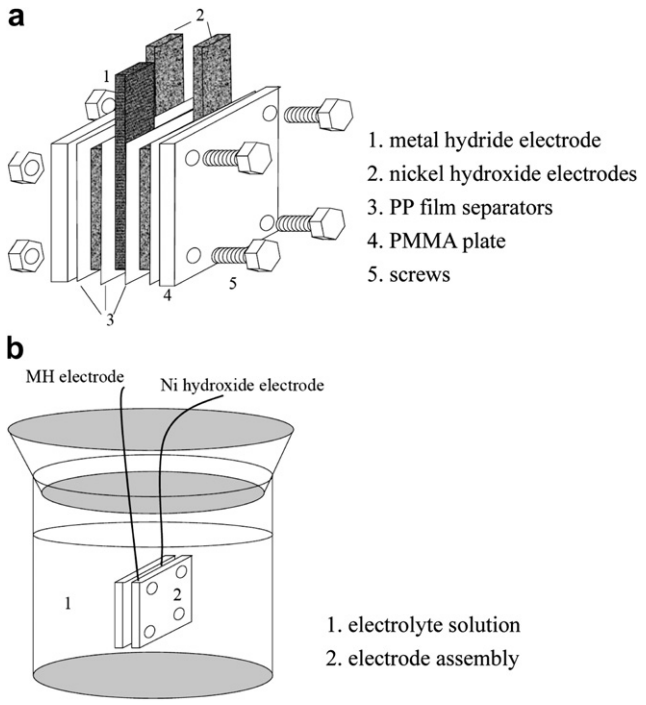

Fig. 1 – Schematic configuration of (a) electrode assembly, and (b) cell of flooded Ni–MH battery.

interactions AB, AC, AD, BC, BD and EF on the responses, which were the Ni loadings and the utilities of the modified MH alloys at various discharge rates. The levels of six control factors and the loadings of Ni on MH alloy (response, y) from the 16 experiments are given in Table 2. The experimental results indicated that the Ni loadings were in the ranges −20.25–10.14% for pH 3.0 and 7.12–11.83% for pH 7.0. For the electroless plating Ni process, by using sodium hypophosphite as the reducing agent, $H_2PO_2^-$ diffused to the surface of the metal hydride substrate and produced adsorbed atomic hydrogen based on the following equations [35]:

Table 2 – L_{16} orthogonal array for electroless plating Ni on MH alloy.

Run No.	A min	B °C	C g	D	E g L^{-1}	F g L^{-1}	y[a] wt%
1	10	70	2	3.0	15	10	2.80
2	10	70	2	7.0	15	30	7.12
3	10	70	4	7.0	30	10	7.80
4	10	70	4	3.0	30	30	4.87
5	10	90	2	3.0	30	10	10.14
6	10	90	2	7.0	30	30	11.83
7	10	90	4	7.0	15	10	9.51
8	10	90	4	3.0	15	30	6.04
9	40	70	2	7.0	30	30	11.26
10	40	70	2	3.0	30	10	0.20
11	40	70	4	3.0	15	30	2.01
12	40	70	4	7.0	15	10	7.70
13	40	90	2	7.0	15	30	8.30
14	40	90	2	3.0	15	10	−20.25
15	40	90	4	3.0	30	30	0.16
16	40	90	4	7.0	30	10	7.80

a The response (y) was the Ni loading on MH alloy.

$$H_2PO_2^- + H_2O \rightarrow HPO_3^- + 2H_{ad} + H^+ \quad (1)$$

$$H_2PO_2^- \rightarrow PO_2^- + 2H_{ad} \quad (2)$$

The nickel ion was reduced by the adsorbed atomic hydrogen and deposited on the substrate

$$Ni^{2+} + 2H_{ad} \rightarrow Ni + 2H^+ \quad (3)$$

As indicated in Eqs. (1)–(3), H^+ formed in the electroless plating Ni and caused a decrease in the pH of the solution. Increasing the pH of the solution resulted in the increase in the electroless plating rate and Ni loading on the MH alloy. Therefore, the Ni loading formed at pH 7.0 was greater than that at pH 3.0. The negative Ni loading for No. 14 in Table 2 revealed that Ni could not be deposited on the alloy. Furthermore, some of the MH alloy was corroded and dissolved in the electroless plating process. The low levels of pH and concentrations of the reducing agent and complex agent (No. 14 conditions in Table 2) were unfavorable to the electroless Ni plating. On the other hand, for the conditions of No. 14, the low level of pH and high level of temperature (90 °C) caused an increase in alloy corrosion. Compared with the unmodified MH alloy, the surface compositions analyzed by EDS for the MH alloy modified by the conditions of No. 14 were changed due to the selective dissolution of the MH alloy elements.

3.2. *Surface morphologies of MH alloy modified by electroless plating Ni*

The unmodified MH alloy, MH alloy modified at pH 3.0 (No. 8 in Table 2) and 7.0 (No. 6 in Table 2), as well as the MH alloy corroded in the electroless plating process (No. 14 in Table 2) were selected to analyze the surface morphologies by SEM (Fig. 2). The smooth surface of the unmodified MH surface (in Fig. 2(a)) was changed to a rougher and fiber-like structure for the MH alloys modified by the conditions of Nos. 6 and 8 (Fig. 2(b) and (c)). Furthermore, compared with the MH alloy modified at pH 3.0 (No. 8, Fig. 2(c)), more roughness and some granular structures of alloy modified at pH 7.0 (No. 6, Fig. 2(b)) were found due to a higher deposition rate at pH 7.0. The Ni deposit texture was not found on the surface of the MH alloy modified under condition No. 14 (Fig. 2(d)). On the other hand, some crevices and potholes caused by corrosion were discovered. The surface morphology of the No. 14 MH alloy correlated well with the negative Ni loading, as shown in Table 2.

The granular deposits were generally found on the surface of the MH alloy modified at pH 7.0, and the Ni and P weight fractions of the deposits analyzed by EDS were obtained as 87.18–92.59% and 7.41–12.82%, respectively. When the MH alloy was modified at pH 3.0, the reliable weight fractions of Ni and P were not obtained due to the EDS analysis of the thinner Ni–P deposit, which was interfered with the MH alloy substrate.

3.3. *Statistical analysis of Ni loading*

The results of the analysis of the variance for electroless plating Ni on MH alloy based on orthogonal array and its

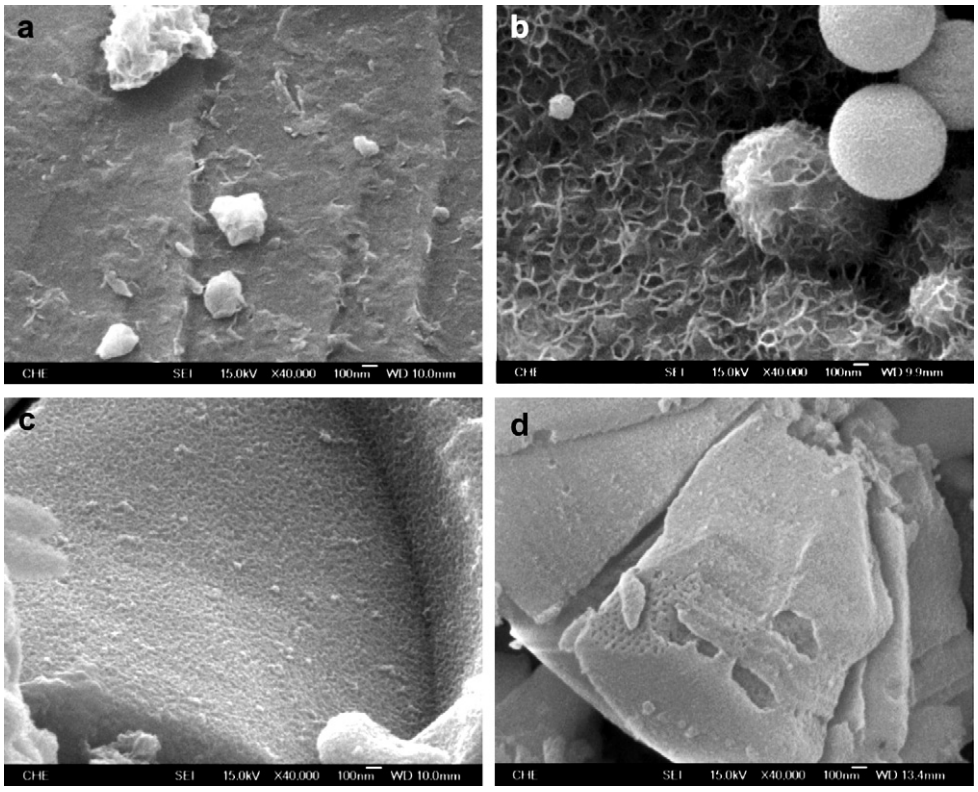

Fig. 2 – Surface morphologies of (a) unmodified MH alloy, and MH alloy modified by conditions of (b) No. 6, (b) No.8, (c) No. 14 in Table 2.

response (Table 2) are illustrated in Table 3. It is common to declare a statistically significant factor if the Pr > F value in Table 3 is less than 0.05 [36]. The experimental and statistical analysis results indicated that the pH value (factor D) was the most important factor with a sum of square equal to 533.83 of the total variance. The effect of factor A (reaction time) was the second most important factor for the electroless plating of Ni on the MH alloy. On the other hand, the effect of reaction temperature (B) and weight of the MH alloy (C) on the Ni loading was not statistically significant since their Pr > F values were greater than 0.05. As for the effect of the two-factor interactions, the most important factor was found to be AD (interaction of reaction time (A) and pH (D)), and the other two-factor interactions shown to be statistically significant included AB, AC, BD, and EF. Only the interaction between the reaction temperature (B) and the weight of the MH alloy (C) exhibited statistical insignificance.

Table 3 – Analysis of variance for the L_{16} orthogonal array measurements with Ni loading as response.

Source	DF	Sum sq.	Mean sq.	F value	Pr > F
A	1	230.37	230.37	28.84	<0.0001
B	1	13.08	13.08	1.64	0.2161
C	1	26.24	26.24	3.29	0.0857
D	1	533.83	533.83	66.82	<0.0001
E	1	118.81	118.81	14.87	0.0011
F	1	83.79	83.79	10.49	0.0043
AB	1	200.90	200.90	25.15	<0.0001
AC	1	59.57	59.57	7.46	0.0133
AD	1	205.34	205.34	25.70	<0.0001
BC	1	19.50	19.50	2.44	0.1347
BD	1	37.63	37.63	4.71	0.0429
EF	1	57.94	57.94	7.25	0.0144
Error	19	151.62	7.98		

The relationships between the response of the system (Ni loading) and the factors analyzed by Duncan's multiple range comparison [37] indicated that a higher Ni loading (response) could be obtained for low level of factors A and B, and high level of factors C, D, E and F. As discussed above, two main reactions occurred within the electroless plating process, i.e., the deposition of Ni and the corrosion of the MH alloy. In the initial stage, the higher deposition rate caused a fast increase in the Ni loading. By increasing the reaction time, the deposition rate decreased due to the exhaustion of the electroless plating reactants. On the other hand, the corrosion of the MH alloy and Ni was increased by increasing the reaction time due to the increase in the concentration of H^+ produced in the electroless plating process (Eqs. (1)–(3)). Hence, a lower Ni loading was obtained for high levels of reaction time and temperature (factors A and B). This inference was further demonstrated by the results in Table 4. When the reaction time increased from 5 to 10 min, the Ni loading increased from 12.02% to a maximum value of 13.09%. The Ni loading decreased to 11.69% by further increasing the time to 30 min. The change in Ni^{2+} concentration and pH value with the reaction time, shown in Table 4, also advocated the inference.

Table 4 – Effect of reaction time on the electroless plating Ni. $T = 80\ ^{\circ}C$, weight of MH alloy = 2 g, initial pH = 7.0, $[NaH_2PO_2] = 30\ g\ L^{-1}$, $[Na_3C_6H_5O_7] = 30\ g\ L^{-1}$.

Reaction time min	Ni loading wt%	$[Ni^{2+}]$ ppm	pH
5	12.02	2230	5.47
10	13.09	2000	5.43
20	12.82	2200	5.43
30	11.69	2300	5.45

3.4. Utilities of MH alloys for Ni–MH batteries discharged at 0.2 C

Using the MH alloy modified by electroless plating Ni with the conditions illustrated in Table 2 as the electroactive materials of the negative electrodes, the Ni–MH batteries were charged with 0.2 C–160% SOC and then discharged at the same C-rate to 0.95 V. The utility of the MH alloy was defined as the ratio of the experimental discharge capacity and the capacity provided by the supplier (310 mAh g^{-1}). The stable utility of the unmodified MH alloy was obtained for a cycle number greater than 3, and the maximum utility was 100.6% for cycle number of 5, as illustrated in Table 5. As illustrated in Fig. 3, at the first charge cycle, the charge potential sharply increased from 1.33 to 1.57 V by increasing the charge time from 0 to 90 min. Further increase the charge time to 480 min the potential changed slightly. For the first discharge cycle, the discharge potential plateau was in the range of 1.30–1.10 V. Hence a high potential difference between the charge and discharge potential plateaus was obtained to be 0.27–0.47 V. The results revealed that a high internal resistance of the battery was found in the first charge/discharge cycle. For the fifth charge/discharge cycle, the components of the Ni–MH battery were completely wetted, and the optimal structures of electrodes were also obtained. Therefore the decrease in the internal resistance of the battery resulted in the significant decrease in the potential difference between the charge and discharge plateaus to about 0.16 V (Fig. 3). The utility of MH alloy hence increased by increasing the charge/discharge cycle from 1 to 5. The similar results were obtained for the modified MH alloys.

For modified MH alloys, stable utilities were achieved by the cycle number of 5, except for the MH alloy modified with condition No. 11, for which a stable utility was obtained for the cycle number of 10. Based on the results in Table 5, the utilities of the MH alloys modified at pH 7.0 were generally greater than those at pH 3.0. The lower utility of the MH alloy modified at pH 3.0 could be explained by less Ni loading and the relatively poor electrical conductivity. Furthermore, the lower utility of the MH alloy modified at pH 3.0 might also be caused by damage to the alloy compositions due to the corrosion occurring with a lower pH solution. The very low utilities of the MH alloys modified by the conditions of Nos. 10, 14 and 15 (Table 2) were mainly due to less Ni loadings, which were found to be 0.20, –20.25 and 0.16%, and the corrosion of alloys. A large amount of the MH alloy corroded in the electroless plating process under the condition of No. 14, resulting in the utility approaching 0% (Table 5).

The relationship between the utility of the modified MH alloys and the electroless plating conditions was statistically analyzed and illustrated in Table 6. For the single factors, the statistically significant factors affecting the utility of the modified MH alloy were the reaction time (A), the weight of

Table 5 – The utility of MH alloy modified by electroless plating Ni at 0.2 C discharge rate. Charging at 0.2 C to 160 SOC%, discharge at 0.2 C to 0.95 V, $T = 30\ ^{\circ}C$, battery soaked at 30 °C for 12 h.

No.[a]	Utility/%				
	Cycle no.				
	1	2	3	4	5
—[b]	84.5 ± 2.3	95.6 ± 0.3	98.6 ± 0.3	99.8 ± 0.1	100.6 ± 0.3
1	29.5 ± 2.4	49.5 ± 2.6	62.5 ± 1.9	69.3 ± 1.6	72.8 ± 1.0
2	88.3 ± 1.2	97.6 ± 0.9	100.2 ± 0.3	101.1 ± 0.5	102.1 ± 0.5
3	80.5 ± 1.5	96.2 ± 1.0	100.9 ± 1.0	101.7 ± 1.3	103.1 ± 1.3
4	65.4 ± 3.2	78.0 ± 1.0	82.8 ± 1.4	85.0 ± 1.4	88.9 ± 1.0
5	54.1 ± 2.1	79.3 ± 1.0	89.7 ± 0.8	93.7 ± 0.4	95.6 ± 0.2
6	85.2 ± 0.5	97.1 ± 0.1	99.1 ± 0.1	100.3 ± 0.3	100.4 ± 0.3
7	84.9 ± 1.0	95.0 ± 0.1	98.6 ± 0.2	100.6 ± 0.4	101.7 ± 0.4
8	59.3 ± 2.8	80.4 ± 3.1	87.5 ± 2.7	90.9 ± 2.6	92.7 ± 2.5
9	88.8 ± 0.8	98.5 ± 0.7	99.9 ± 0.5	100.6 ± 0.3	100.6 ± 0.1
10	12.7 ± 1.0	13.3 ± 1.1	12.1 ± 0.2	12.6 ± 0.6	14.7 ± 1.3
11	20.4 ± 0.1	28.2 ± 1.4	34.4 ± 2.2	40.6 ± 2.2	46.5 ± 2.9
	58.0 ± 0.4($6^{\$}$)	60.4 ± 0.5($7^{\$}$)	63.6 ± 0.04($8^{\$}$)	65.4 ± 0.3($9^{\$}$)	66.8 ± 1.0($10^{\$}$)
12	80.7 ± 0.7	96.9 ± 0.4	101.3 ± 0.1	101.7 ± 0.2	102.3 ± 0.3
13	89.1 ± 0.7	97.7 ± 0.5	99.2 ± 0.5	99.7 ± 0.6	100.1 ± 0.2
14	0.4 ± 0.1	0.6 ± 0.04	0.7 ± 0.03	0.9 ± 0.1	1.0 ± 0.03
15	14.3 ± 1.9	17.0 ± 2.2	19.9 ± 2.0	22.5 ± 0.2	25.1 ± 2.4
16	88.8 ± 1.0	95.9 ± 0.7	96.2 ± 0.2	96.2 ± 0.5	96.4 ± 0.4

a The conditions for modifying MH alloy were given in Table 2.
b Unmodified MH alloy; $ cycle number for greater than 5.

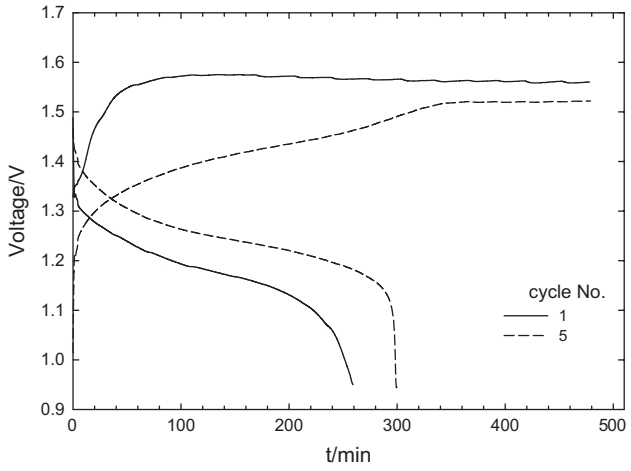

Fig. 3 – Charge/discharge curves of Ni-unmodified MH battery. T = 30 °C, soaking time = 12 h, charge at 0.2 C to 160% SOC.

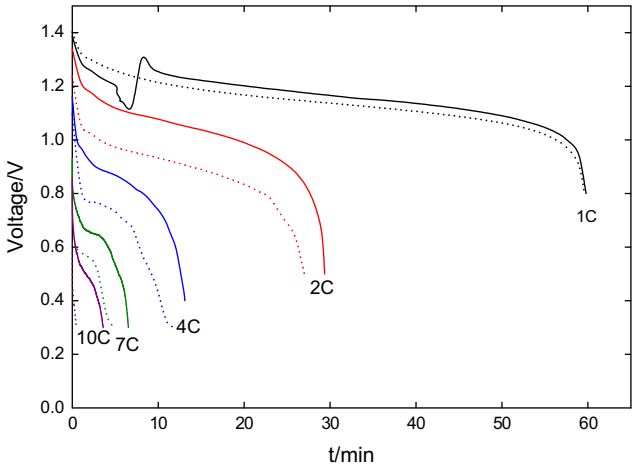

Fig. 4 – Discharge curves of Ni–MH batteries for various discharge rates. ⋯: unmodified MH alloy, —: MH alloy modified by No. 2 conditions (Table 2). T = 30 °C, soaking time = 12 h, charge at 0.2 C to 140% SOC.

MH alloy (C), pH (D), and the concentration of the complex agent (F). The analysis results also revealed that the most important factor was the pH of the solution, with a contribution equal to 43.96% of the total variance. Except for the factor of BD (interaction of reaction temperature and pH), all of the other two-factor interactions had statistically significant effects on the utility of the modified MH alloy.

Based on the analysis using Duncan's multiple range comparison, the low levels of reaction time, reaction temperature and reducing agent, as well as the high levels of weight of the MH alloy, pH and the concentration of the complex agent favored the utility of the MH alloy discharged at 0.2 C. All of these suggestive factor levels, except for pH, indicated that a lower Ni deposition rate could obtain a higher MH alloy utility in Ni–MH batteries. A lower Ni deposition rate resulted in a denser structure and increased the electrical conductivity and utility of the MH alloy. As described above, for a lower pH, the alloy was corroded and resulted in the decrease in the utility of the material.

Table 6 – Analysis of variance for the L_{16} orthogonal array measurements with MH alloy utility at discharge rate of 0.2 C.

Source	DF	Sum sq.	Mean sq.	F Value	Pr > F
A	1	7812.81	7812.81	181.27	<0.0001
B	1	184.37	184.37	4.28	0.0525
C	1	994.69	994.69	23.08	0.0001
D	1	15216.84	15216.84	353.06	<0.0001
E	1	25.90	25.90	0.60	0.4478
F	1	983.57	983.57	22.82	0.0001
AB	1	907.49	907.49	21.06	0.0002
AC	1	426.39	426.39	9.89	0.0053
AD	1	6862.35	6862.35	159.22	<0.0001
BC	1	335.34	335.34	7.78	0.0117
BD	1	47.56	47.56	1.10	0.3067
EF	1	774.31	774.31	17.97	0.0004
Error	19	818.90	43.10		

3.5. *Utilities of MH alloys for Ni–MH batteries with higher discharge rates*

The discharge curves of the unmodified MH alloy and the MH alloy modified by the condition of No. 2 (Table 2) for various discharge rates are shown in Fig. 4. The results revealed that the decrease in the discharge plateau voltage with the discharge rate was mainly due to the increase in the charge-transfer and mass-transfer overpotentials and ohmic

Table 7 – The utility of MH alloy modified by electroless plating Ni at higher discharge rate. Charging at 0.2 C to 160 SOC%, T = 30 °C, battery soaked at 30 °C for 12 h.

No.[a]	Utility/%				
	Discharge rate				
	1C	2C	4C	7C	10C
——[b]	98.8 ± 0.5	89.8 ± 0.2	67.1 ± 0.5	51.5 ± 4.8	7.6 ± 0.3
1	78.7 ± 1.3	74.9 ± 1.3	66.2 ± 1.4	37.8 ± 1.1	15.4 ± 1.6
2	101.3 ± 1.6	98.9 ± 1.0	89.1 ± 1.7	75.7 ± 0.6	58.7 ± 1.2
3	105.7 ± 1.1	101.6 ± 1.0	89.9 ± 1.3	73.1 ± 2.9	51.6 ± 1.1
4	86.3 ± 1.0	71.9 ± 1.9	59.7 ± 0.3	34.0 ± 1.0	12.9 ± 2.3
5	99.7 ± 1.9	92.2 ± 1.9	84.2 ± 0.4	68.7 ± 0.8	46.3 ± 0.8
6	102.6 ± 2.0	94.0 ± 0.1	82.8 ± 4.9	60.0 ± 2.4	51.7 ± 0.6
7	100.0 ± 1.7	95.3 ± 1.8	77.7 ± 3.6	61.0 ± 3.4	17.5 ± 2.5
8	91.9 ± 1.1	89.1 ± 2.6	74.6 ± 0.2	48.5 ± 0.7	13.4 ± 1.5
9	98.8 ± 1.2	94.7 ± 3.0	78.8 ± 1.7	54.3 ± 1.1	13.3 ± 0.2
10	10.6 ± 2.1	8.4 ± 1.6	4.6 ± 0.2	2.0 ± 0.8	0.5 ± 0.4
11	65.1 ± 0.6	63.1 ± 0.2	46.9 ± 2.0	19.7 ± 3.1	1.7 ± 0.8
12	95.0 ± 2.8	91.4 ± 1.6	80.3 ± 3.2	51.0 ± 1.3	20.5 ± 1.4
13	101.6 ± 1.3	98.7 ± 1.0	86.9 ± 4.0	65.6 ± 2.5	31.0 ± 2.4
14	0.3 ± 0.1	0.4 ± 0.2	0.4 ± 0.3	0.5 ± 0.4	0.5 ± 0.5
15	20.8 ± 0.7	18.5 ± 0.3	7.9 ± 0.7	1.5 ± 1.3	0.1 ± 0.1
16	90.9 ± 3.8	88.0 ± 2.1	72.9 ± 0.2	56.0 ± 0.6	35.6 ± 4.7

a The conditions for modifying MH alloy were given in Table 2.
b Unmodified MH alloy.

Table 8 – Analysis of variance for the L_{16} orthogonal array measurements with MH alloy utility at discharge rate of 10 C.

Source	DF	Sum sq.	Mean sq.	F Value	Pr > F
A	1	3380.27	3380.27	453.20	<0.0001
B	1	60.64	60.64	8.13	0.0102
C	1	521.56	521.56	69.93	<0.0001
D	1	4476.70	4476.70	600.20	<0.0001
E	1	358.25	358.25	48.03	<0.0001
F	1	3.37	3.37	0.45	0.5093
AB	1	206.30	206.30	27.66	<0.0001
AC	1	1003.63	1003.63	134.56	<0.0001
AD	1	4.27	4.27	0.57	0.4585
BC	1	481.51	481.51	64.56	<0.0001
BD	1	176.96	176.96	23.72	0.0001
EF	1	1425.11	1425.11	191.07	<0.0001
Error	19	141.70	7.46		

potential drop. However, the discharge plateau voltage of the battery based on the modified MH alloy was significantly greater than that of the unmodified MH alloy for various discharge rates (Fig. 4). The results were inferred to the higher electric conductivity and the anti-oxidation of the MH alloy modified by the Ni deposit.

The utilities of the MH alloy modified by the conditions shown in Table 2 with various discharge rates are summarized in Table 7. When increasing the discharge rate from 1 to 10 C, the utility of the unmodified MH alloy decreased from 98.8 to 7.6%. In comparison with the unmodified MH alloy, the utilities of the modified MH alloys were generally promoted at higher discharging rates, except for the modified MH alloys with lower Ni loadings, i.e., the alloys modified by the conditions of Nos. 10, 11, 14 and 15 in Table 2. The maximum utility at the discharge rate of 10 C was obtained to be 58.7% for the MH alloy modified with the No. 2 condition, as shown in Table 2.

The analysis of the variance results with the utilities of the modified MH alloy at the discharge rate of 10 C are summarized in Table 8. The results revealed that the single factors of A, B, C, D and E, and the two-factor interactions of AB, AC, BC, BD and EF exhibited statistical significance on the utility of the modified MH alloy at a discharging rate of 10 C. The Duncan's multiple range comparison showed that the higher utility of the modified MH at 10 C discharging rate was obtained for the low levels of factors A (reaction time), C (weight of MH alloy) and F (concentration of complex agent), as well as the high levels of factors B (reaction temperature), D (pH value) and E (concentration of reducing agent), which resulted in a higher Ni depositing rate. A higher Ni depositing rate caused a rougher morphology of the deposit and increased the diffusion rate through the deposit layer on the modified MH alloy. As a result, the utility of the modified MH alloy at a higher discharge rate was increased by increasing the Ni depositing rate.

4. Conclusions

$MmNi_{3.81}Mn_{0.41}Al_{0.19}Co_{0.76}$ (MH alloy) was modified by the electroless plating of Ni based on the two-level orthogonal array $L_{16}(2^{15})$, which was designed and analyzed with six factors and six two-factor interactions. The Ni loading on the MH alloy prepared at a low pH level (pH 3.0) was significantly less than that at a high pH level (pH 7.0). Statistical analysis revealed that the most important single factor and two-factor interaction for obtaining a higher Ni loading were the factors D (pH of solution) and AD (interaction of reaction time and pH). When the utility of the modified MH alloys at a lower discharging rate (0.2 °C) as a response to the statistical analysis, higher utilities were obtained with the modifying factors set for a lower Ni depositing rate, i.e., the low levels of factors A, B (reaction temperature) and E (concentration of reducing agent), as well as the high levels of factors C (weight of MH alloy), D and F (concentration of complex agent). On the other hand, statistical analysis suggested that the higher utility of the MH alloy at a high discharging rate (10 C) was obtained with a higher Ni depositing rate, i.e., the low levels of factors A, C and F, as well as the high levels of factors B, D and E. The denser Ni deposit obtained for the lower depositing rate resulted in higher electrical conductivity of the Ni deposit, which favored the utility of the MH alloy at a lower discharging rate. For the Ni–MH battery discharged at a high rate, the utility of the MH alloy was strongly affected by the diffusion rate of the substances. Therefore, a rougher deposit on the MH alloy modified with a higher Ni depositing rate favored the diffusion rate and the utility of the alloy.

Acknowledgment

The financial support of National Science Council of the Republic of China (Project number: NSC 98-2218-E-029-004) is acknowledged.

REFERENCES

[1] Abu-Sharkh S, Arnold RJ, Kohler J, Li R, Markvart T, Ross JR, et al. Can microgrids make a major contribution to UK energy supply? Renewable and Sustainable Energy Reviews 2006;10:78–127.
[2] Fetcenko MA, Ovshinsky SR, Reichman B, Young K, Fierro C, Koch J, et al. Recent advances in NiMH battery technology. Journal of Power Sources 2007;165:544–51.
[3] Raju M, Ananth MV, Vijayaraghavan L. Influence of electroless coatings of Cu, Ni–P and Co–P on $MmNi_{3.25}Al_{0.35}Mn_{0.25}Co_{0.66}$ alloy used as anodes in Ni–MH batteries. Journal of Alloys and Compounds 2009;475:664–71.
[4] Feng F, Northwood DO. Effect of surface modification on the performance of negative electrodes in Ni/MH batteries. International Journal of Hydrogen Energy 2004;29:955–60.
[5] Parimala R, Ananth MV, Ramaprabhu S, Raju M. Effect of electroless coating of Cu, Ni and Pd on $ZrMn_{0.2}V_{0.2}Fe_{0.8}Ni_{0.8}$ alloy used as anodes in Ni–MH batteries. International Journal of Hydrogen Energy 2004;29:509–13.
[6] Choi SJ, Choi J, Seo CY, Park CN. An electroless copper plating method for Ti, Zr-based hydrogen storage alloys. Journal of Alloys and Compounds 2003;356-357:725–9.
[7] Deng C, Shi P, Zhang S. Effect of surface modification on the electrochemical performances of $LaNi_5$ hydrogen storage alloy in Ni/MH batteries. Materials Chemistry and Physics 2006;98:514–8.

[8] Manimaran K, Ananth MV, Raju M, Renganathan NGM, Ganesan M, Nithya G. Electrochemical investigations on cobalt-microencapsulated $MmNi_{2.38}Al_{0.82}Co_{0.66}Si_{0.77}Fe_{0.13}Mn_{0.24}$ hydrogen storage alloys for Ni–MH batteries. International Journal of Hydrogen Energy 2010;35:4630–7.
[9] Chen J, Zhang Y. Nickel/metal hydride batteries using microencapsulated hydrogen storage alloy. International Journal of Hydrogen Energy 1995;20:235–7.
[10] Zhao X, Ma L, Gao Y, Ding Y, Shen X. Effect of surface treatments on microstructure and electrochemical properties of La–Ni–Al hydrogen storage alloy. International Journal of Hydrogen Energy 2009;34:1904–9.
[11] Jenq SN, Yang HW, Wang YY, Wan CC. Modification of $Ti_{0.35}Zr_{0.65}Ni_{1.2}V_{0.6}Mn_{0.2}$ alloy powder by electroless nickel coating and its influence on discharge performance. Journal of Power Sources 1995;57:111–8.
[12] Wu MS, Wu HR, Wang YY, Wan CC. Surface treatment for hydrogen storage alloy of nickel/metal hydride battery. Journal of Alloys and Compounds 2000;302:248–57.
[13] Jenq SN, Yang HW, Wang YY, Wan CC. Discharge performance of $Ti_{0.35}Zr_{0.65}Ni_{1.2}V_{0.6}Mn_{0.2}$ alloy electrode modified by electroless nickel plating. Materials Chemistry and Physics 1997;48:10–6.
[14] Wu MS, Wu HR, Wang YY, Wan CC. Electrochemical investigation of hydrogen-storage alloy electrode with duplex surface modification. International Journal of Hydrogen Energy 2004;29:1263–9.
[15] Li Y, Han S, Liu Z. Effect of Mo–Ni treatment on electrochemical kinetics of La–Mg–Ni-based hydrogen storage alloys. International Journal of Hydrogen Energy 2010;35:12858–63.
[16] Kim SH, Lee SM, Lee PS, Lee JY. A study on the electrode characteristics of V-Ti alloy surface-modified by ballmilling process. Journal of The Electrochemical Society 2001;148(7): A696–700.
[17] Lee SM, Kim SH, Lee JY. A study on the electrode characteristics of Zr-based alloy surface-modified with Ti-based alloy by ball-milling process as an anode material for Ni–MH rechargeable batteries. Journal of Alloys and Compounds 2002;330–332:796–801.
[18] Kim JH, Lee H, Lee PS, Seo CY, Lee JY. A study on the improvement of the cyclic durability by Cr substitution in V–Ti alloy and surface modification by the ball-milling process. Journal of Alloys and Compounds 2003;348:293–300.
[19] Lee SM, Yu JS, Lee PS, Lee JY. Application of flake metal as a surface modifier for the hydrogen absorbing intermetallic electrode of an Ni–MH rechargeable battery. Materials Science and Engineering 2002;A329–331:339–45.
[20] Tang R, Liu Y, Zhu J, Yu G. Electrochemical properties of Co-free $Ml_{0.8}Mg_{0.2}Ni_{3.4}Al_{0.4}$ hydrogen storage alloy ballmilled with Ni and Mo. Journal of The Electrochemical Society 2004; 151:A1774–7.
[21] Yu XB, Wu Z, Huang TS. Improved electrochemical performance of BCC alloy by Ni addition and surface modification with AB_5 alloy. Journal of Alloys and Compounds 2009;476:787–90.
[22] Wu DC, Li L, Liang GY, Guo YL, Wu HB. Improved electrochemical properties of amorphous $Mg_{65}Ni_{27}La_8$ electrodes: surface modification using graphite. Journal of Power Sources 2009;189:1251–5.
[23] Sakintuna B, Lamari-Darkrim F, Hirscher M. Metal hydride materials for solid hydrogen storage: a review. International Journal of Hydrogen Energy 2007;32:1121–40.
[24] Xu Y-H, Wang G, Chen C-P, Wang Q-D, Wang X. The structure and electrode properties of non-stoichiometric$A_{1.2}B_2$ type C14 Laves alloy and the effect of surface modification. International Journal of Hydrogen Energy 2007;32:1050–8.
[25] Yang K, Wu F, Chen S, Zhang CZ. Effect of surface modification of metal hydride electrode on performance of MH/Ni batteries. Transactions of Nonferrous Metals Society of China 2007;17:200–4.
[26] Yang K, Chen S, Wu F. Study on the surface modification of metal hydride electrodes with cobalt. Journal of Power Sources 2008;184:617–21.
[27] Davids MW, Lototskyy M, Nechaev A, Naidoo Q, Williams M, Klochko Y. Surface modification of TiFe hydrogen storage alloy by metal-organic chemical vapour deposition of palladium. International Journal of Hydrogen Energy 2011;36: 9743–50.
[28] Ding H, Han S, Liu Y, Hao J, Li Y, Zhang J. Electrochemical performance studies on cobalt and nickel electroplated La–Mg–Ni-based hydrogen storage alloys. International Journal of Hydrogen Energy 2009;34: 9402–8.
[29] Law HH, Vyas B, Zahurak SM, Kammlott GW. A novel plating process for microencapsulating metal hydrides. Journal of The Electrochemical Society 1996;143: 2596–601.
[30] Sakai T, Ishikawa H, Oguro K, Iwakura C, Yoneyama H. Effects of microencapsulation of hydrogen storage alloy on the performances of sealed nickel/metal hydride batteries. Journal of The Electrochemical Society 1987;134: 558–62.
[31] Iwakura C, Kajiya Y, Yoneyama H, Sakai T, Oguro K, Ishikawa H. Self-discharge mechanism of nickel-hydrogen batteries using metal hydride anodes. Journal of The Electrochemical Society 1989;136:1351–5.
[32] Lundstedt T, Seifert E, Abramo L, Thelin B, Nystrom A, Pettersen J, et al. Experimental design and optimization. Chemometrics and Intelligent Laboratory Systems 1998;42: 3–40.
[33] Wang T-Y, Huang C-Y. Improving forecasting performance by employing the Taguchi method. European Journal of Operational Research 2007;176:1052–65.
[34] Ross PJ. Taguchi techniques for Quality Engineering. McGraw-Hill Book Company; 1988.
[35] Ying HG, Yan M, Ma TY, Wu JM, Yu LQ. Effects of NH_4F on the deposition rate and buffering capability of electroless Ni–P plating solution. Surface & Coatings Technology 2007;202: 217–21.
[36] Wahdame B, Candusso D, Francois X, Harel F, Kauffmann J-M, Coquery G. Design of experiment techniques for fuel cell characterization and development. International Journal of Hydrogen Energy 2009;34:967–80.
[37] Christensen R. Analysis of variance, design and Regression: applied statistical Methods. Chapman & Hill; 1996.